Available online at www.sciencedirect.com

SciVerse ScienceDirect

Ceramics International 39 (2013) 6223–6228

CERAMICS INTERNATIONAL

www.elsevier.com/locate/ceramint

Structural, electric and multiferroic properties of Sm-doped $BiFeO_3$ thin films prepared by the sol–gel process

Xue Xu, Tan Guoqiang*, Ren Huijun, Xia Ao

Key Laboratory of Auxiliary Chemistry & Technology for Chemical Industry, Ministry of Education, Shaanxi University of Science & Technology, Xi'an 710021, China

Received 14 December 2012; received in revised form 12 January 2013; accepted 14 January 2013
Available online 23 January 2013

Abstract

Pure polycrystalline $Bi_{1-x}Sm_xFeO_3$ (BSFO) ($x=0$–0.12) thin films were successfully prepared on FTO/glass substrates by the sol–gel method. The influence of Sm doping on the structure, dielectric, leakage current, ferroelectric and ferromagnetic properties of the BSFO films was investigated. X-ray diffraction analysis and FE-SEM images both reveal a gradual rhombohedra to pseudo-tetragonal phase transition with the increase of Sm dopant content. On one hand, a proper amount of Sm doping can decrease the leakage current densities of the BSFO thin films. On the other hand, excess Sm substitution for Bi will lead to multiphase coexistence in the film, the lattice inhomogeneity results in more defects in the film, which can increase the leakage current density. The result shows that defects in the complexes lead to electric domain back-switching in the $BSFO_{x=0.06}$ thin film, resulting in a decreased dielectric constant, leakage current and remanent polarization. The $BSFO_{x=0.09}$ thin film is promising in practical application because of its highest dielectric constant, remanent polarization and remanent magnetization of 203–185, 70 $\mu C/cm^2$ and 1.31 emu/cm^3, respectively.

Keywords: $BiFeO_3$; Sm-doping; Multiferroic; Phase transition

1. Introduction

Multiferroic materials which exhibit coexistence of (anti)ferroelectricity, (anti)ferromagnetism, and/or ferroelasticity in a certain range of temperatures have attracted much attention [1]. $BiFeO_3$ (BFO) is a typical single phase multiferroic material with distorted perovskite structure, belonging to *R*3*c* space lattice [2]. Its Curie temperature (T_C) is 1103 K while Neel temperature (T_N) is 643 K [3]. BFO has been widely used in magnetoelectric sensors, self-spinning electronic devices and non-volatile storage [4]. It is the only known material with robust multiferroicity above room temperature and is of great scientific interest for that reason [5]. At present, there are some vulnerabilities existing in pure BFO that hinders its real applications. On one hand, it is very easy to have the valence change of Fe and volatilization of Bi when annealing, resulting in high leakage current in the film. On the other hand, low dielectric constant and electrical resistivity in the BFO makes it difficult to observe the saturated electric hysteresis loops [6,7].

For preparation of BFO films with the sol–gel method, properties improvement is mainly focused on dopant modification, i.e. rare element (*RE*) substitution for Bi ions in pure BFO lattice. Many researches on *RE*-doped (*RE*= La, Eu, Sm) BFO thin films were reported in the past few years. La-doped BFO thin film was transformed from pseudo-cubic into tetragonal phase, resulting in both increased ferroelectric and ferromagnetic properties [8]. Eu-doped BFO thin film was transformed from *R*3*c* rhombohedra into *Pbnm* triclinic structure, the $Bi_{0.9}Eu_{0.1}FeO_3$ thin film exhibited a big remanent polarization and small coercive strength of 74 $\mu C/cm^2$ and 250 kV/cm, respectively [9]. In the Cheng's study, the morphotropic phase boundary (MPB) appeared at 14% Sm dopant, its coercive field was decreased and piezoelectric constant reached to a maximum value of 160 pm/V [10]. For rare element substitution whose ionic radius is different from

*Corresponding author. Tel.: +86 137 5987 8391.
E-mail address: tan3114@163.com (T. Guoqiang).

0272-8842/$ - see front matter © 2012 Elsevier Ltd and Techna Group S.r.l. All rights reserved.
http://dx.doi.org/10.1016/j.ceramint.2013.01.042

Bi^{3+} ion, the spacing between Bi^{3+} and Fe^{3+} ions and long-range ferroelectric order in the BFO are both changed, resulting in enhancement of spontaneous polarization (P_s).

As discussed above, many researches have studied ferroelectric and piezoelectric properties of the BFO thin films by adjusting *RE* doping concentration, but few researches have investigated the ferromagnetic properties. In this work, we fabricated BFO and Sm-substituted BFO (BSFO) films on FTO/glass substrate using stoichiometric sol–gel solution and annealed the films at 550 °C in atmosphere to avoid the formation of impurities. Sm-doped BFO thin films have been prepared on FTO/glass substrate. The effects of different Sm dopant contents on the structure, ferroelectric and ferromagnetic properties of the BSFO thin films are investigated and discussed.

2. Experimental procedure

Raw materials $Sm(NO_3)_3 \cdot 6H_2O$, $Fe(NO_3)_3 \cdot 9H_2O$ and $Bi(NO_3)_3 \cdot 5H_2O$ with a proportion of (0∼0.12):1:(1.05∼0.93) (5 mol% of excess Bi was added to compensate for bismuth loss during the heat treatment) were dissolved in 2-methoxyethanol and some acetic anhydride was added to dehydrate and adjust the pH value of the solution. Then the proper amount of 2-methoxyethanol was used to adjust the precursor solution concentration to 0.3 mol/L. After stirring the solution for 1 h, a stable precursor solution was obtained. FTO/glass substrate was washed in acetone, alcohol and deionized water in proper order. The precursor solution was spin coated on the FTO/glass substrates at 4000 rpm for 15 s. After spun-coating, thin films were pre-annealed at 350 °C for 5 min and subsequently annealed at 550 °C for 5 min in atmosphere for crystallization. This process was repeated several times to obtain the desired film thickness. Au top electrode was of 0.502 mm^2 sputtered on the surface of the thin films with a mask on the top. After annealing at 300 °C for 20 min, the electrode can completely contact with the film. A capacitor is obtained, and it is ready for electric properties tests.

Japan Rigaku Company D/max-2200 X-ray diffractometer was used to identify the structure and crystallinity of the thin films. With Cu target, the scanning step length was 0.02° and operated at 40 kV and 20 mA. FE-SEM (JEOL JSM-6700) and atomic force microscopy (NT-MDT: Model Ntegra) were used to observe the surface morphologies of the films. The dielectric properties of the films were tested by Agilent E4980A Concise LCR meter, the electric hysteresis loops and leakage current densities of the films were measured by aixACCT TF-Analyzer 2000, and the magnetic properties of the films were analyzed by the MPMS-XL-7 superconducting quantum interference magnetic measuring system.

3. Result and discussion

Fig. 1 shows XRD patterns of the BFO and BSFO thin films. The BFO film is polycrystalline perovskite structure without any parasitic phase and matches well with the JCPDS card number 71-2494. The X-ray analysis reveals rhombohedrally distorted perovskite-type cell with lattice constants $a_{hex}=5.588$ Å and $c_{hex}=13.867$ Å. The space group is determined to be $R3c$ with six formula units per hexagonal unit cell. Since Sm^{3+} has a smaller ionic radius of 0.964 Å compared to Bi^{3+} ionic radius of 1.03 Å, the compression stress generated from small ionic substitution for Bi makes the BSFO lattice shrink, as a consequence of decreased interplanar spacing. As shown in the inset of Fig. 1, the diffraction peaks shifting to high degree of 2θ confirm that interplanar spacing in the BSFO films is decreased (according to Bragg equation $2d \sin\theta = n\lambda$). It is also seen that (110) peak is partially overlapped with (104) peak in the $BSFO_{x=0.03}$ film, and overlapped completely in the $BSFO_{x=0.09}$ film. The diffraction peak right shifting and overlapping like this both indicate a gradual phase transition process from the rhombohedral to pseudo-tetragonal with Sm doping content increasing from 0 to 0.12 [11,12]. The same phase transition process has also been early reported in Mn doped BFO films [13]. Fig. 1(b) plots unit cell parameters of the BSFO thin films as a function of the Sm doping contents. The (110) interplanar

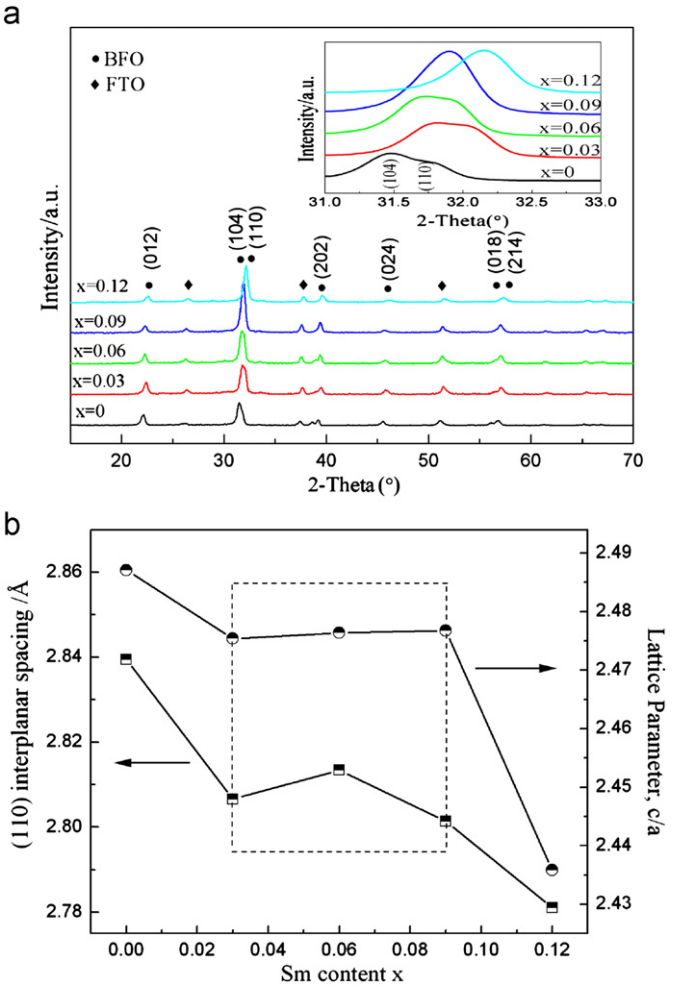

Fig. 1. XRD patterns of $Bi_{1-x}Sm_xFeO_3$ films at room temperature. (a) XRD patterns of $Bi_{1-x}Sm_xFeO_3$ films at the range of 31°–33°; (b) unit cell parameter of $Bi_{1-x}Sm_xFeO_3$ thin films as a function of Sm doping content.

spacing and lattice parameter c/a of the BSFO films are both decreased compared to that of the BFO film. Within the limits of Sm doping content 0.03–0.09, (110) interplanar spacing and lattice parameter c/a are both changed slightly, indicating that the structures of the $BSFO_{x=0.03–0.09}$ films are gradually changed with the increase of Sm doping content. The $BSFO_{x=0.03–0.09}$ films are located at a multiphase coexistence state [14,15], may be associated with the gradually increased triclinic phase [16]. Because of the limited X-ray diffraction peaks, the presence of multiphase structures cannot be separately ascertained.

Fig. 2 shows surface micrographs of the BFO and BSFO thin films and AFM image of the $BSFO_{x=0.09}$ thin film. Obviously, the BFO and $BSFO_{x=0.12}$ film both exhibit a well crystallized microstructure as well as a smooth surface. In contrast, the $BSFO_{x=0.03–0.09}$ films show gradually decreased grain size and inhomogeneous surface micrographs. In particular, when the Sm doping content increase to 0.09, structure transition leads to two kinds of grains in the $BSFO_{x=0.09}$ film. One is big grains with ups and downs protruded in a certain direction as shown in the AFM image of the $BSFO_{x=0.09}$ film in Fig. 2(f). The other is small grains dispersed among the big ones as shown in Fig. 2(d). The extraordinary grain growth showed results from the mismatching between $BiFeO_3$ and $SmFeO_3$ in the BSFO lattice, and further proved multiphase coexistence in the $BSFO_{x=0.09}$ thin film.

Fig. 3 shows dielectric constant (ε_r) and dielectric loss ($\tan\delta$) of the BFO and BSFO films at the measured frequency ranging from 1 KHz to 1 MHz at room temperature. It is found that ε_r does not increase monotonously with the increase of Sm dopant content. The ε_r value of the BFO and BSFO films measured at 1 MHz is 95, 130, 80, 185 and 150. The dielectric constants do not show monotonous change with the increase of Sm dopant content which indicates that the amount of Sm dopant plays an important role in varying the defect concentration, such as O^{2-} vacancies, Bi^{3+} vacancies and Fe^{2+} concentration in the film. This is further confirmed by leakage current properties of the BSFO films shown in Fig. 4. These defects can be polarized in the electric field so as to increase the dielectric constant of the BSFO films. Considering that the $BSFO_{x=0.06}$ film has a minimum ε_r of 80

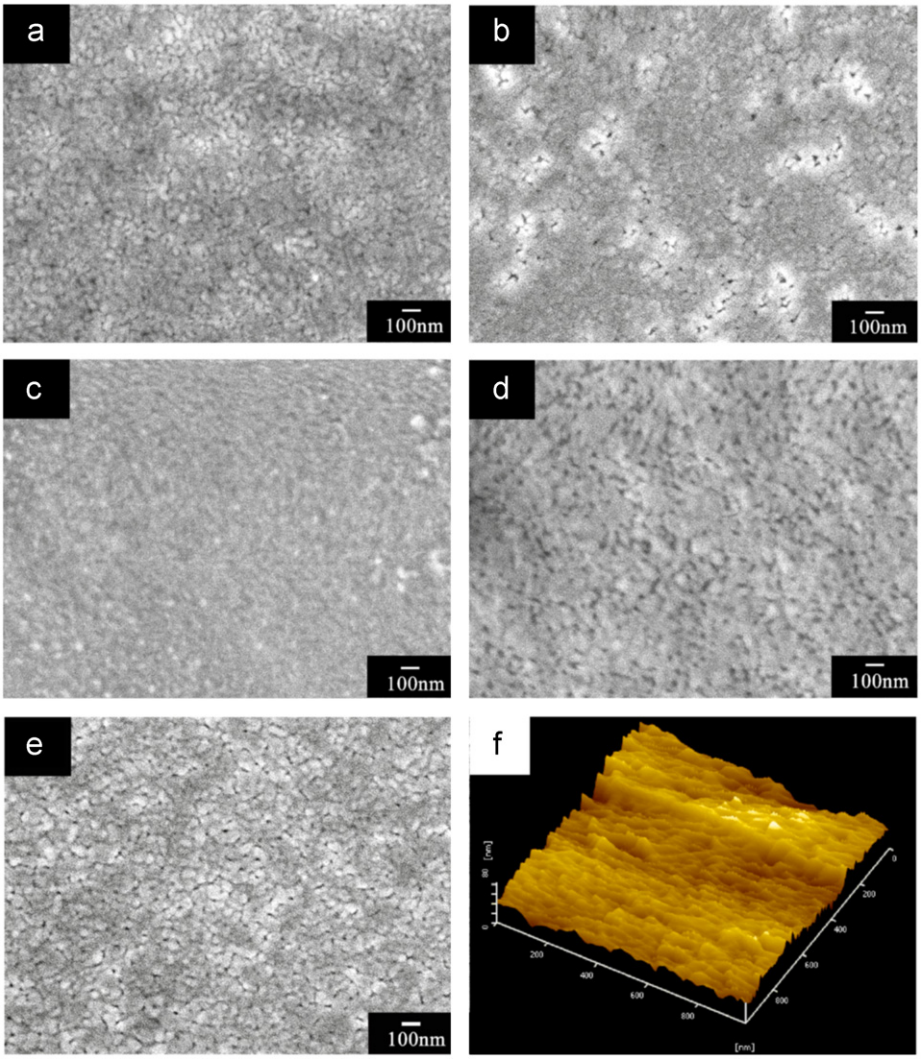

Fig. 2. FE-SEM images and AFM image of $Bi_{1-x}Sm_xFeO_3$ films (a) $x=0$, (b) $x=0.03$, (c) $x=0.06$, (d) $x=0.09$, (e) $x=0.12$, and (f) $x=0.09$.

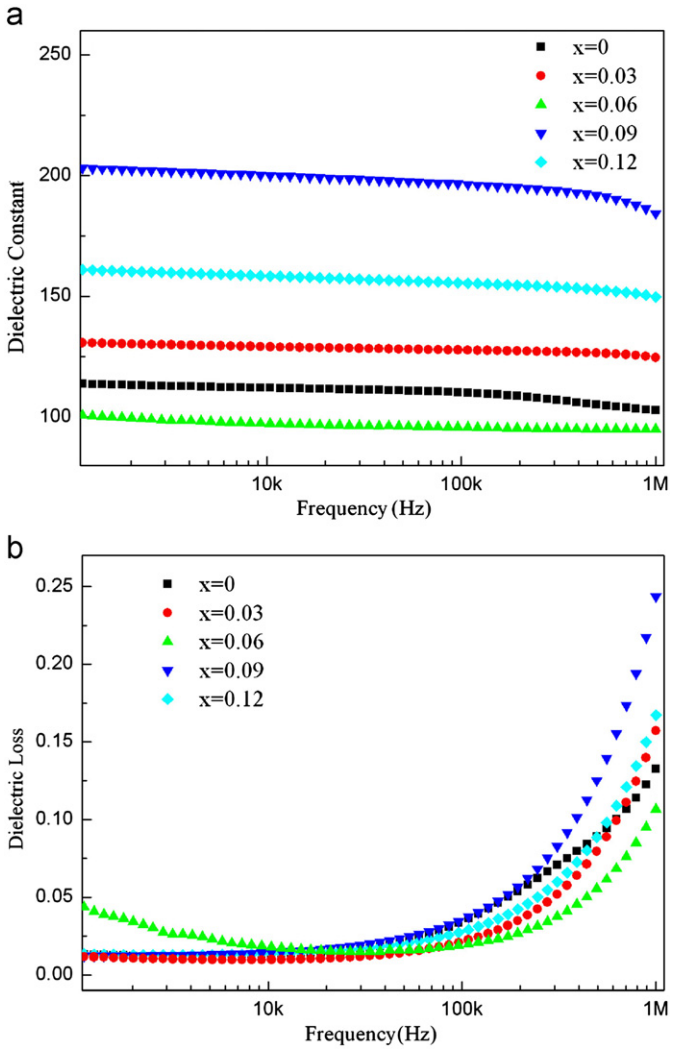

Fig. 3. (a) Dielectric constant and (b) dielectric loss of $Bi_{1-x}Sm_xFeO_3$ films as a function of frequency at room temperature.

at 1 MHz, whereas the $BSFO_{x=0.09}$ film has a maximum ε_r of 185 at 1 MHz, there may be more defects existing in the $BSFO_{x=0.09}$ film. The decreased electric constant of the $BSFO_{x=0.12}$ film is attributed to its single phase and lower defect concentration in the lattice. In Fig. 3(b), the dielectric losses of the BSFO films are kept below 0.05 at a low frequency of 1–100 kHz. The dielectric losses increase above 100 kHz is due to the dipole inertia [17]. When the frequency reaches to 1 MHz, the $BSFO_{x=0.06}$ film has the lowest dielectric loss of 0.10 compared to the highest dielectric loss of 0.24 for the $BSFO_{x=0.09}$ film, which is also attributed to the defect concentration in each film. As defect plays an important role in affecting leakage current density, while the leakage current density is a crucial factor in affecting dielectric loss, the sudden increase of dielectric loss for the $BSFO_{x=0.09}$ film is attributed to its highest leakage current density caused by multiphase coexistence.

Fig. 4 shows the leakage current density as a function of electric field for the BFO and BSFO thin films measured at room temperature. The leakage current densities of the BSFO films show the same varying law as their dielectric constant with the increase of Sm doping content. The leakage current density of $BSFO_{x=0.03}$ is slightly increased compared to that of the BFO film which is 2.95×10^{-4} A/cm^2 at an electric field of 200 kV/cm. As Sm doping content increases from 0.06 to 0.12, the leakage current density is 7.5×10^{-5} A/cm^2, 2.5×10^{-3} A/cm^2 and 1.1×10^{-3} A/cm^2 at the electric field of 200 kV/cm. The lowest leakage current density for the $BSFO_{x=0.06}$ film further confirms that there are less defects in the $BSFO_{x=0.06}$ film. On the contrary, the highest leakage current density for the $BSFO_{x=0.09}$ film must be attributed to more defects in its lattice. The defect generated by structure transition plays a key role in affecting the leakage current density of the film. On one hand, a proper amount of Sm doping can decrease the leakage current densities of the BSFO thin films. On the other hand, excess Sm substitution for Bi will lead to multiphase coexistence in the film and the lattice inhomogeneity results in more defects in the film, which can increase the leakage current density.

Fig. 5 plots the polarization–electric field (P–E) hysteresis loops for the BFO and BSFO films measured under the maximum electric field of 510 KV/cm at 1 kHz. The $BSFO_{x=0–0.06}$ films show a lossy type P–E loops because of their low dielectric constants, and particularlly reveal that less than 6% Sm dopant cannot improve the ferroelectric property of the BFO film. The remanent polarization (P_r) is 1.5, 3.1, 0.7 μC/cm^2. The $BSFO_{x=0.06}$ film has the lowest P_r, which is attributed to its electric domain back-switching mechanism [18]. Electric domain back-switching mechanism is related to big amounts of defective complexes, such as $(V_O^{2-})^{\bullet\bullet}$–$(Fe^{2+}Fe^{3+})'$, which perform as a partial electric field, resulting in electric domain back-switching and decreased spontaneous polarization [18]. When Sm doping content increases to 0.09, the enhanced remanent polarization of 70 μC/cm^2 is observed compared to that of 41 μC/cm^2 in the $BSFO_{x=0.12}$ film. As known to all, large ferroelectric order and spontaneous polarization in

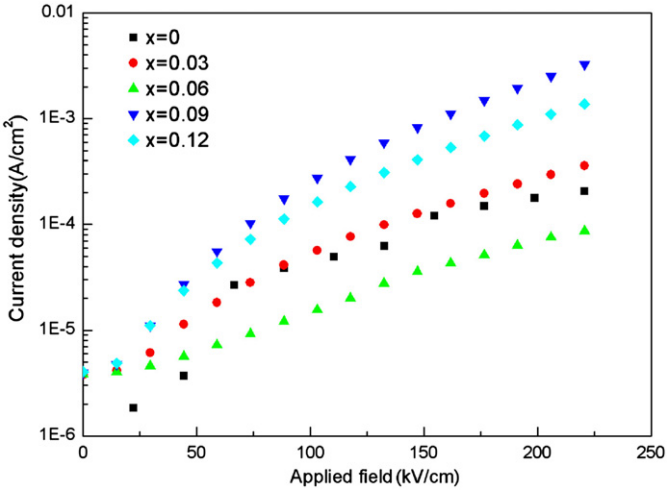

Fig. 4. Leakage currents density of $Bi_{1-x}Sm_xFeO_3$ films as a function of applied voltage at room temperature.

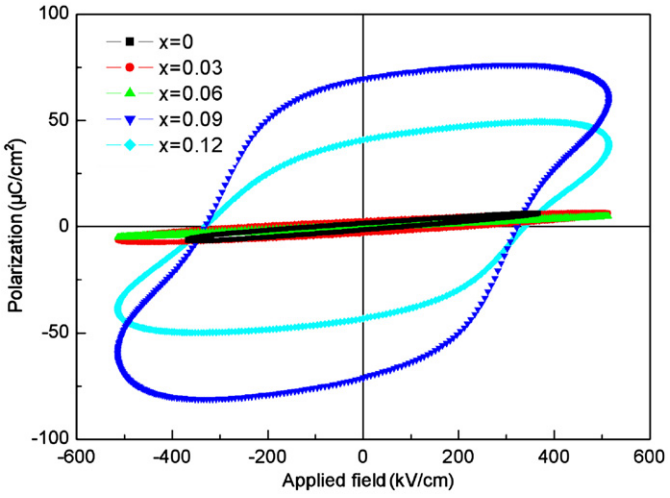

Fig. 5. Electric hysteresis loops of $Bi_{1-x}Sm_xFeO_3$ films as a function of applied voltage measured at room temperature.

BFO primarily results from the stereochemically active $6s^2$ lone pairs on the Bi^{3+} ions [19]. Thus, systematic substitution to replace the Bi^{3+} ions with smaller Sm^{3+} dopant will not only change the spacing between Bi^{3+}/Sm^{3+} ions and iron–oxygen octahedral, but also alter the long-range ferroelectric order. Videlicet, 9% Sm dopant substitution for Bi ions could adequately release the ferroelectric of the BFO film. Furthermore, both $BSFO_{x=0.09}$ and $BSFO_{x=0.12}$ films exhibit a poor rectangular P–E loops that may be attributed to their high leakage current densities.

The room temperature magnetic hysteresis (M–H) loops for the BFO and BSFO thin films are shown in Fig. 6(a), which are measured using MPMS-XL-7 superconducting quantum interference magnetic measuring system at the maximum magnetic field of 10 kOe. Fig. 6(b) illustrates the remanent magnetization (M_r) and saturated magnetization (M_s) of the films as a function of Sm doping contents. As Sm doping content increases from 0 to 0.12, the M_r and M_s of the films become 0.63, 0.48, 0.67, 1.31, 0.70 emu/cm^3 and 4.3, 4.2, 10.5, 7.3, 3.9 emu/cm^3, respectively. Compared with the BFO film, Sm doping can both increase M_r and M_s; the $BSFO_{x=0.06}$ film has a maximum M_s of 10.5 emu/cm^3 and the $BSFO_{x=0.09}$ film has a maximum M_r of 1.31 emu/cm^3. The M_r and M_s values are both dramatically decreased when the Sm doping content increases to 0.12. This might be attributed to the structure transformation, a pseudo-tetragonal structure for the $BSFO_{x=0.12}$ film. It is well known that the increase in the macroscopic magnetization of BFO-based materials is attributed to either destroyed spatially homogeneous spin-modulated structure, or the increased spin canting angle [20]. Considering that both M_r and M_s are Sm doping content dependent, the macroscopic magnetization in the BFO film must be cycloid in structure and long-range ferromagnetic order controlled. Structure transition of the BSFO films can destroy the homogeneous spin structure; therefore the latent magnetization locked within the cycloid structure is released, resulting in the enhancement of macroscopic magnetization. In addition,

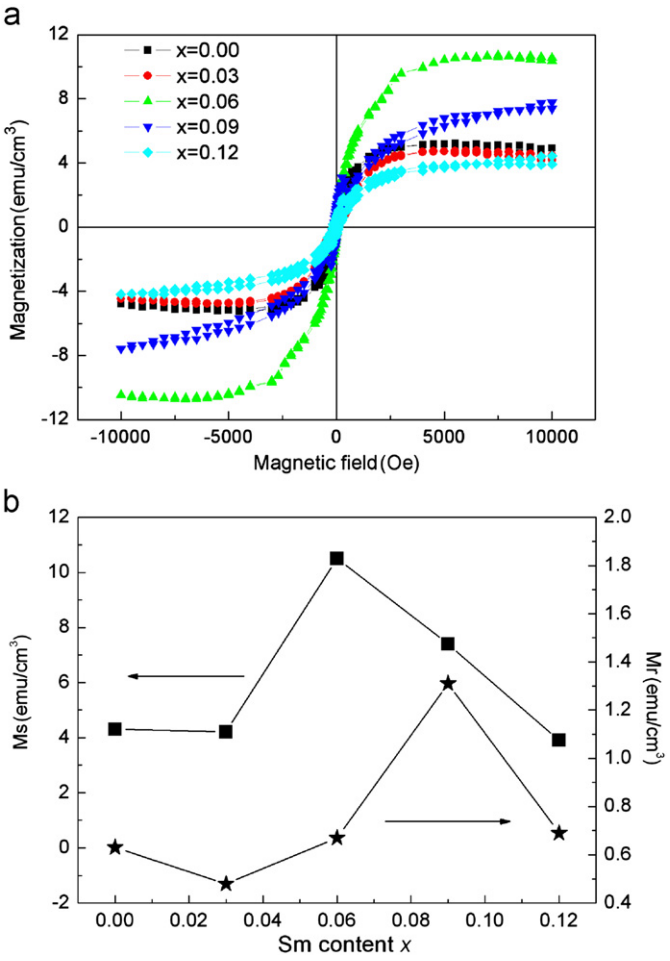

Fig. 6. (a) Magnetic hysteresis loops of $Bi_{1-x}Sm_xFeO_3$ films; (b) M_s and M_r of $Bi_{1-x}Sm_xFeO_3$ films as a function of Sm doping content.

the highest remanent magnetization in the $BSFO_{x=0.09}$ film may also be attributed to the spin interaction between Sm^{3+} and Fe^{3+} or Fe^{2+} ions, and the great amount of Fe^{2+} caused by multiphase coexistence. The existence of Fe^{2+} ions would possibly cause a double exchange interaction between Fe^{2+} and Fe^{3+} ions through oxygen, which may result in the enhancement of ferromagnetism [21].

4. Conclusion

In summary, polycrystalline BSFO thin films were prepared on FTO/glass substrates by the sol–gel method. The effects of Sm doping on the structure, dielectric, leakage current, ferroelectric and ferromagnetic properties of the BSFO films were investigated. X-ray diffraction analysis and FE-SEM images both reveal a gradual rhombohedra to pseudo-tetragonal phase transition with the increase of Sm dopant content. The leakage current densities of the BSFO films show the same varying law as their dielectric constants with the increase of Sm doping content. The defective complexes in the $BSFO_{x=0.06}$ film lead to electric domain back-switching, a decreased remanent polarization of 0.7 μC/cm^2 is observed, whereas the

$BSFO_{x=0.06}$ film shows enhanced ferromagnetic property with a maximum saturation magnetization of 10.5 emu/cm^3. The $BSFO_{x=0.09}$ thin film exhibits the maximum remanent polarization of 70 $\mu C/cm^2$ and remanent magnetization of 1.31 emu/cm^3. Substitution of Bi^{3+} ions with smaller Sm^{3+} dopant will not only change the spacing between Bi^{3+}/Sm^{3+} ions and iron–oxygen octahedral, but also alter the long-range ferroelectric order. Nine percent Sm substitution for Bi ions could adequately release the ferroelectric of the BFO film. In addition, the enhancement of remanent magnetization for the $BSFO_{x=0.09}$ is attributed to its great amount of Fe^{2+} and supressed periodic self-spinning structure.

Acknowledgments

This work is supported by the Project of the National Natural Science Foundation of China (Grant no. 51172135); the Young Scientists Fund of the National Natural Science Foundation of China (Grant no. 51002092); the Research and special projects of the Education Department of Shaanxi Province (Grant no. 12JK0445); and the Graduate Innovation Fund of Shaanxi University of Science and Technology (Grant no. SUST-A04).

References

[1] N.A. Spaldin, M. Fiebig, The renaissance of magnetoelectric multiferroics, Science 309 (2005) 391.
[2] J. Zhu, W.B. Luo, Y.R. Li, Growth and properties of $BiFeO_3$ thin films deposited on $LaNiO_3$-buffered $SrTiO_3$ (001) and (111) substrates by PLD, Applied Surface Science 255 (2008) 3466.
[3] T. Karthik, A. Srinivas, V. Kamaraj, V. Chandrasekeran, Influence of in-situ magnetic field pressing on the structural and multiferroic behaviour of $BiFeO_3$ ceramics, Ceramics International 38 (2012) 1093.
[4] M. Fiebig, Th. Lottermoser, D. Fröhlich, A.V. Goltsev, R.V. Pisarev, Observation of coupled magnetic and electric domains, Nature 419 (2) (2002) 818.
[5] W. Siemons, G.J. MacDougall, A.A. Aczel, J.L. Zarestky, M.D. Biegalski, S. Liang, E. Dagotto, S.E. Nagler, H.M. Christen, Strain dependence of transition temperatures and structural symmetry of $BiFeO_3$ within the tetragonal-like structure, Applied Physics Letters 101 (2012) 212901.
[6] J. Wang, J.B. Neaton, H. Zheng, V. Nagarajan, S.B. Ogale, B. Liu, D. Viehland, V. Vaithyanathan, D.G. Schlom, U.V. Waghmare, N.A. Spaldin, K.M. Rabe, M. Wuttig, R. Ramesh, Epitaxial $BiFeO_3$ multiferroic thin film heterostructures, Science 299 (2003) 1719.
[7] J.K. Kim, S.S. Kim, W.-J. Kim, A.S. Bhalla, Substitution effects on the ferroelectric properties of $BiFeO_3$ thin films prepared by chemical solution deposition, Journal of Applied Physics 101 (2007) 014108.
[8] D. Lee, M.G. Kim, S. Ryu, H.M. Jang, Epitaxially grown La-modified $BiFeO_3$ magnetoferroelectric thin films, Applied Physics Letters 86 (2005) 222903.
[9] Z.Q. Hu, M. Li, J. Liu, L. Pei, J. Wang, B.F. Yu, X.Z. Zhao, Structural transition and multiferroic properties of Eu-doped $BiFeO_3$ thin films, Journal of the American Ceramic Society 93 (2010) 2743.
[10] C.-J. Cheng, D. Kan, S.-H. Lim, W.R. McKenzie, P.R. Munroe, L.G. Salamanca-Riba, R.L. Withers, I. Takeuchi, V. Nagarajan, Structural transitions and complex domain structures across a ferroelectric-to-antiferroelectric phase boundary in epitaxial Sm-doped $BiFeO_3$ thin films, Physical Review B 80 (2009) 014109.
[11] G.D. Hu, X. Cheng, W.B. Wu, C.H. Yang, Effects of Gd substitution on structure and ferroelectric properties of $BiFeO_3$ thin films prepared using metal organic decomposition, Applied Physics Letters 91 (2007) 232909.
[12] J. Liu, M. Li, L. Pei, J. Wang, B. Yua, X. Wanga, X. Zhao, Structural and multiferroic properties of the Ce-doped $BiFeO_3$ thin films, Journal of Alloys and Compounds 493 (2010) 544.
[13] S.K. Singh, H. Ishiwara, K. Sato, K. Maruyama, Microstructure and frequency dependent electrical properties of Mn-substituted $BiFeO_3$ thin films, Journal of Applied Physics 102 (2007) 094109.
[14] R. Guo, L.E. Cross, S.E. Park, B. Noheda, D. Cox, G. Shirane, Origin of the high piezoelectric response in $PbZr_{1-x}Ti_xO_3$, Physical Review Letters 84 (2000) 235423.
[15] W.G. Chen, W. Ren, L. You, Y.R. Yang, Z.H. Chen, Y.J. Qi, X. Zou, J.L. Wang, T. Sritharan, P. Yang, L. Bellaiche, L. Chen, Domain structure and in-plane switching in a highly strained $Bi_{0.9}Sm_{0.1}FeO_3$ film, Applied Physics Letters 99 (2011) 222904.
[16] G.L. Yuan, Siu Wing Or, J.M. Liu, Z.G. Liu, Structural transformation and ferroelectromagnetic behavior in single-phase $Bi_{1-x}Nd_x$-FeO_3 multiferroic ceramics, Applied Physics Letters 89 (2006) 052905.
[17] H.R. Liu, Z.L. Liu, X.L. Li, X.G. Li, K. Yao, $Bi_{1-x}La_xFeO_3$ films on $LaNiO_3$ bottom electrode by the sol–gel process, Journal of Physics D: Applied Physics 40 (2007) 242.
[18] X.M. Chen, G.D. Hu, W.B. Wu, C.H Yang, X. Wang, S.H. Fan, Large piezoelectric coefficient in Tb-doped $BiFeO_3$ films, Journal of the American Ceramic Society 93 (2010) 948.
[19] H.M. Christen, J.H. Nam, H.S. Kim, A.J. Hatt, N.A. Spaldin, Stress-induced R–M_A–M_C–T symmetry changes in $BiFeO_3$ films, Physical Review B 83 (2011) 144107.
[20] Z. Quan, W. Liu, H. Hu, S. Xu, S. Bobby, G.J. Fang, M. Li, X.Z. Zhao, Microstructure, electrical and magnetic properties of Ce-doped $BiFeO_3$ thin films, Journal of Applied Physics 104 (2008) 084106.
[21] F. Huang, X. Lu, W. Lin, X. Wu, Y. Kan, J. Zhu, Effect of Nd dopant on magnetic and electric properties of $BiFeO_3$ thin films prepared by metal organic deposition method, Applied Physics Letters 89 (2006) 242914.